Design of phase-shifting algorithms by fine-tuning spectral shaping

A. Gonzalez,[1] M. Servin,[1,*] J. C. Estrada,[1] and J. A. Quiroga[2]

[1]*Centro de Investigaciones en Optica A.C., Loma del bosque 115, Col. Lomas del Campestre, Leon Guanajuato, 37150 Mexico*

[2]*Optics Department, Universidad Complutense de Madrid, Facultad de CC. Físicas, Ciudad Universitaria s/n, 28040 Madrid, Spain*

**mservin@cio.mx*

Abstract: To estimate the modulating wavefront of an interferogram in Phase Shifting Interferometry (PSI) one frequently uses a Phase Shifting Algorithm (PSA). All PSAs take as input *N* phase-shifted interferometric measures, and give an estimation of their modulating phase. The first and best known PSA designed explicitly to reduce a systematic error source (detuning) was the 5-steps, Schwider-Hariharan (*SH*-PSA) PSA. Since then, dozens of PSAs have been published, designed to reduce specific data error sources on the demodulated phase. In Electrical Engineering the Frequency Transfer Function (FTF) of their linear filters is their standard design tool. Recently the FTF is also being used to design PSAs. In this paper we propose a technique for designing PSAs by fine-tuning the few spectral zeroes of a PSA to approximate a template FTF spectrum. The PSA's spectral zeroes are moved (tuned) while gauging the plot changes on the resulting FTF's magnitude.

OCIS codes: (120.3180) Interferometry; (120.2650) Fringe analysis.

References and links

1. J. Schwider, R. Burow, K. E. Elssner, J. Grzanna, R. Spolaczyk, and K. Merkel, "Digital wave-front measuring interferometry: some systematic error sources," Appl. Opt. **22**(21), 3421–3432 (1983).
2. P. Hariharan, B. F. Oreb, and T. Eiju, "Digital phase-shifting interferometry: a simple error-compensating phase calculation algorithm," Appl. Opt. **26**(13), 2504–2506 (1987).
3. D. Malacara, M. Servin, and Z. Malacara, *Interferogram Analysis for Optical Testing* (Taylor & Francis, CRC, 2005).
4. K. Freischlad, and C. L. Koliopoulos, "Fourier description of digital phase-measuring interferometry," J. Opt. Soc. Am. A **7**(4), 542–551 (1990).
5. K. G. Larkin, and B. F. Oreb, "Design and assessment of symmetrical phase-shifting algorithms," J. Opt. Soc. Am. A **9**(10), 1740–1748 (1992).
6. J. Schwider, O. Falkenstörfer, H. Schreiber, H. Zöller, and N. Streibl, "New compensating four-phase algorithm for phase-shift interferometry," Opt. Eng. **32**(8), 1883–1885 (1993).
7. P. Groot, "Derivation of algorithms for phase-shifting interferometry using the concept of a data-sampling window," Appl. Opt. **34**(22), 4723–4730 (1995).
8. J. Schmit, and K. Creath, "Window function influence on phase error in phase-shifting algorithms," Appl. Opt. **35**(28), 5642–5649 (1996).
9. Y. Surrel, "Design of algorithms for phase measurements by the use of phase stepping," Appl. Opt. **35**(1), 51–60 (1996).
10. J. G. Proakis, and D. G. Manolakis, *Digital Signal Processing*, 4th ed. (Prentice Hall, 2007).
11. J. Burke, "Extended averaging phase-shifting schemes for Fizeau interferometry on high-numerical aperture spherical surfaces," Proc. of SPIE **7790**, (2010).
12. M. Servin, J. C. Estrada, and J. A. Quiroga, "The general theory of phase shifting algorithms," Opt. Express **17**(24), 21867–21881 (2009).

1. Introduction

Schwider et al. [1] derived the first (and best known) 5-steps detuning-robust PSI algorithm, and afterwards Hariharan et al. [2] further analyzed its properties. In the book of Malacara et al. [3] an encyclopedic number of PSI algorithms are presented, including the motivation behind many of them; their spectral plots are also shown according to Freischlad and

#143799 - $15.00 USD Received 7 Mar 2011; revised 25 Apr 2011; accepted 25 Apr 2011; published 17 May 2011

Koliopoulos (F&K) [4]. Spectral analysis of PSAs was popularized only after the F&K paper [4] was published. Nowadays, spectral analysis is the gold-standard reference to compare among several PSAs. Most people uses this spectra to visualize and gauge among several promising PSAs, and choose the best one for their needs [4–8,11,12].

More recently Surrel proposed an x-polynomial $P(x)$ associated with a PSA named the Characteristic Polynomial (CP) [9]. The x-polynomial closely follows the z-transform, or in Surrel's words [9]: "This introduction of a polynomial is similar to what is underlying in the z-transform theory". That is probably why Surrel preferred the use of x instead of z for his $P(x)$ polynomial. Then, Surrel proposed the CP-diagram, to visualize some properties of a PSA based on the (discrete) angular location over the unit circle of these zeroes and their multiplicities [9]. Surrel proposed no continuous spectral plot to gauge his x-polynomials [9], as the F&K spectral plot does provide [4]. He did not follow the standard continuous spectral analysis of z-transformed digital filters [10].

In 2010, Burke [11] efficiently combined both perspectives: the discrete CP-diagram [9], and the continuous F&K spectral analysis [4]. Burke did this to point-out the importance of fine-tuning the zeroes of a x-polynomial of *symmetric* PSAs. That is, Burke generated a new visualizing-gauging technique, by combining the discrete CP-diagram [9], with the F&K continuous spectrum [4,11], while finely tuning the PSA' symmetric spectral zeroes.

However, as demonstrated in [12], one drawback of the F&K's spectral analysis [4] is that it changes when the PSI algorithm's reference carrier (the local oscillator) is rotated. Another important drawback of the F&K spectrum is that *only symmetrical PSAs may be F&K spectrally analyzed*. That is because, F&K analysis needs to: "*analyze the spectrum without constant or common phase factors* [1]", and in this way obtain two real functions to plot. We repeat, the F&K spectral analysis can only be made if the PSA is symmetric, such as the ones analyzed by Burke [11], and Larkin *et al.* [5], and others [3]. As a consequence, general (non-symmetric) PSAs simply cannot be spectrally analyzed using F&K. Briefly, the F&K spectral plot limitations are: a) The spectral plot changes when the local oscillator is phase shifted [12], and b) F&K cannot plot the PSA's spectra of general *non-symmetric* PSAs. These two drawbacks are serious limitation of the F&K spectral analysis technique.

A different perspective of the PSA's theory just discussed was proposed by Servin et al. [12]. In this paper a general theory of PSAs based on the Frequency Transfer Function (FTF) $H(\omega)$ is given. The FTF is just the Fourier transform of the impulse response of a digital filter $h(t)$, that is $H(\omega)=F[h(t)]$ [10]; where $F[\cdot]$ is the Fourier transform. The use of the FTF however new in PSI, has been the standard way of spectral analysis in signal processing engineering for decades [10]. The spectral analysis of PSAs based on the FTF does not have the limitations of the F&K spectral analysis.

The CP and the FTF perspectives are mathematically equivalent. The x-polynomial follows closely the z-transform of $h(t)$, while the FTF is the Fourier transform of $h(t)$; both perspectives are related by $x=e^{i\omega}$ [10]. The discrete CP-diagram associated with the x-polynomial only shows the CP's zeroes and their multiplicities. In other words, the CP-diagram shows the behaviour of $H(\omega)$ only at the neighborhood of the level set $H(\omega)=0$. In contrast the plot of $|H(\omega)|$ give the continuous, full visualization, of the spectral shape; including the zeroes shown in a CP-diagram. In short, the CP-diagram is a visual subset of $H(\omega)$, representing only its behaviour near $H(\omega)=0$. Note that Surrel [9] could have used the continuous FTF spectral plot $|P(e^{i\omega})|$ for gauging his x-polynomials, but he did not. Therefore, a CP-diagram does not provide the full visualizing information provided by $|H(\omega)|$. As a consequence, it is difficult to use the CP-diagram for fine-tuning the few zeroes in a PSA. The detailed (continuous) spectral plot provided by $|H(\omega)|$, is paramount to fine-tuning the spectral-shape, as our examples below show. We need to visualize and gauge the subtle changes in the shape of $|H(\omega)|$ (magnitude of the FTF), to finely tune the PSA' spectral zeroes to approximate a target spectrum. Finally note that, the target spectrum may be estimated by spectral estimation of experimentally obtained fringe patterns. This real-data spectral estimation, and the desired phase noise-rejection are the key to know the size N of the PSA.

#143799 - $15.00 USD Received 7 Mar 2011; revised 25 Apr 2011; accepted 25 Apr 2011; published 17 May 2011

In this paper, just to build a conceptual bridge, we have adopted a combined CP-FTF visualization. But given that the CP-diagram is a visual subset of our $|H(\omega)|$ plot, we would not need the CP-diagram, all the PSA's information is within our $|H(\omega)|$ continuous plot.

2. Spectral analysis of PSI algorithms based on the FTF

For the reader's convenience, we briefly review the FTF approach in PSI [12]. Let us show the standard mathematical model of a set of N phase-shifted interferometric data as,

$$I(x,y,t)=\sum_{k=0}^{N-1}\{a(x,y)+b(x,y)\cos[\varphi(x,y)+\omega_0 k]\}\,\delta(t-k)\,. \tag{1}$$

where the background illumination is $a(x,y)$, the fringe contrast is $b(x,y)$, and the carrier frequency is ω_0 (radians/interferogram). The Fourier transform $F[\bullet]$ of this signal over t is,

$$I(x,y,\omega)=a\delta(\omega)+\frac{b}{2}\exp[-i\varphi]\,\delta(\omega+\omega_0)+\frac{b}{2}\exp[i\varphi]\,\delta(\omega-\omega_0). \tag{2}$$

To know the interesting phase $\varphi(x,y)$ one needs a filter $h(t)$, to wipe-out the $a\delta(\omega)$ term and one $b/2$ term. To this end, the measured signal $I(t)$ is introduced into a general N-steps PSA as,

$$\tan[\varphi(x,y)]=\frac{\sum_{k=0}^{N-1}a_k\sin(\omega_0 t)I(k)}{\sum_{k=0}^{N-1}a_k\cos(\omega_0 t)I(k)}\quad. \tag{3}$$

This PSA may be seen as the following N-steps, quadrature-filter $h(t)$ tuned at ω_0 rad/sample,

$$h(t)=\left\{\sum_{k=0}^{N-1}a_k\delta(t-k)\right\}e^{i\omega_0 t},\qquad H(\omega)=F[h(t)]=\sum_{k=0}^{N-1}a_k e^{-ik(\omega-\omega_0)}. \tag{4}$$

The data $I(t)$ in Eq. (1) and the quadrature-filter $h(t)$ may be convolved as,

$$S=\left[I(t)*h(t)\right]_{t=N-1}=\sum_{k=0}^{N-1}a_k e^{i\omega_0 k}I(k)\,. \tag{5}$$

The complex number S is the value of $I(t)*h(t)$ evaluated at the middle-point $t=N$-1, in which the filter $h(t)$ and the data $I(t)$ fully overlap. Finally, the searched phase is $\varphi(x,y)=angle[S]$.

We visualize and gauge the PSA spectrum's amplitude shape by plotting $|H(\omega)|$ as [12],

$$\left|H(\omega)\right|=\left|F[h(t)]\right|=\sqrt{Re(\omega)^2+Im(\omega)^2}\,. \tag{6}$$

where $H(\omega)=Re(\omega)+i\,Im(\omega)$, being $Re(\omega)$ and $Im(\omega)$ real-valued functions. The magnitude of $H(\omega)$ has the good properties of being invariant to local oscillator's ($\exp[i\omega_0 t]$) phase-shifts, and have a well-defined spectral plot for either a symmetric or non-symmetric PSAs.

3. Characteristic polynomial (CP) associated to a PSI algorithms

The CP proposed by Surrel [9] is defined from the right hand side of Eq. (5) as,

$$P(x)=\sum_{k=0}^{N-1}a_k e^{i\omega_0 k}x^k=\prod_{k=0}^{N-2}(x-d_k)\,. \tag{7}$$

$P(x)$ is the CP x-polynomial, the data $I(k)$ in Eq. (5) is formally substituted by x^k [9]. As Surrel shows, it is convenient to express $P(x)$ as a product of N-1 monomials $(x-d_k)$. M roots at d_k means that the PSA is robust to detuning at d_k up to order M. Finally, the zeroes d_k, and their

#143799 - $15.00 USD Received 7 Mar 2011; revised 25 Apr 2011; accepted 25 Apr 2011; published 17 May 2011

multiplicities are plotted in a CP-diagram [9]. First-order zeroes are plotted as small solid disks, and their multiplicities with greater circles around them [9].

Note that the FTF and CP analyzing perspectives are related by,

$$H(\omega) = e^{-i(N-1)\omega} P(e^{i\omega}) . \tag{8}$$

Given that the x-polynomial $P(x)$ is closely related with the z-transform, this mathematical equivalence (Eq. (8)) has been known for decades in digital linear system's theory [10].

4. Fine-tuning spectral-zeroes for approximating a desired PSA spectrum

A first-order linear system that generates a (first-order) spectral zero at ω_0 is [10],

$$h(t) = [\delta(t) - \delta(t-1)]\, e^{-i\omega_0 t}. \tag{9}$$

This may readily be seen by Fourier transforming $h(t)$ as,

$$H(\omega) = F[h(t)] = 1 - e^{-i(\omega+\omega_0)}. \tag{10}$$

This is the basic building-block of our zero-based, spectral-shaping design of PSAs. Note that, the equivalent x-monomial is $P(x)=[x-\exp(-i\omega_0)]$. We will combine several first-order blocks (Eq. (10)), freely tuning their zeroes, to approximate a desired PSA spectral template.

As a first example, suppose we want a 5-step PSA's having a flatter rejecting-band around $-\pi/2$ than a 5-step Schwider-Hariharan (*SH*) PSA [1,2]. The *SH*-PSA has the following FTF,

$$H_{SH}(\omega) = (1-e^{i\omega})\left[\, 1 - e^{-i(\omega+\pi/2)} \,\right]^2 [1 - e^{-i(\omega+\pi)}]. \tag{11}$$

The x-polynomial of the *SH*-PSA is $(x\text{-}1)(x+i)^2(x+1)$. The CP-diagram and the plot of $|H_{SH}(\omega)|$ are shown in Fig. 1. This PSA has a second-order zero at $-\pi/2$, and two first-order zeroes at 0 and π. The second-order zero gives (second-order) detuning robustness at $-\pi/2$.

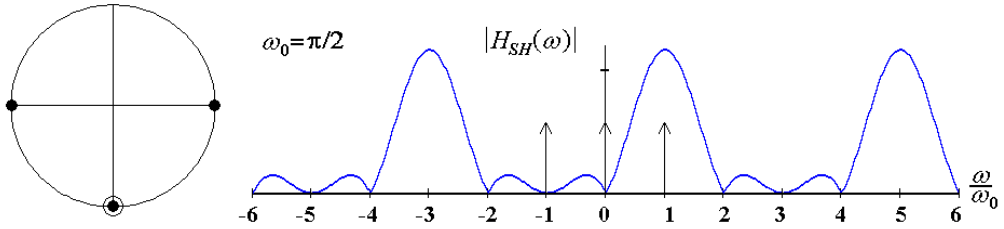

Fig. 1. Magnitude of $H_{SH}(\omega)$ Eq. (11), and its CP-diagram. The PSA' spectral plot $|H_{SH}(\omega)|$ has two first-order zeroes at 0, and π, and a second-order one at $-\pi/2$.

We now freely move and fine-tune (by trial and error) one zero at $-\pi/2$, and the one at π, to flatten the response around $-\pi/2$. This is done while gauging the $|H_5(\omega)|$ plot. After some iterations we settle on the following FTF, which corresponds to a non-symmetric PSA,

$$H_5(\omega) = (1-e^{i\omega})[\,1 - e^{-i(\omega+0.45\omega_0)}][\,1 - e^{-i(\omega+\omega_0)}][\,1 - e^{-i(\omega+1.4\omega_0)}]. \tag{12}$$

The equivalent (CP) x-polynomial is $P_5(x) = (x-1)(x-e^{-i\,0.225\pi})(x-e^{-i\,0.5\pi})(x-e^{-i\,0.7\pi})$. The CP-diagram and the plot of $|H_5(\omega)|$ are shown in Fig. 2. By inverse-Fourier transforming $H_5(\omega)$, or expanding $P_5(x)$, (both options being equally easy) we find the desired *non-symmetric* PSA as,

$$\tan[\phi] = \frac{-2.4I(\pi/2) + 2.9I(\pi) + 0.57I(3\pi/2) - I(2\pi)}{I(0) - 1.2I(\pi/2) - 2.3I(\pi) + 2.7I(3\pi/2) - 0.23I(2\pi)}. \tag{13}$$

#143799 - $15.00 USD Received 7 Mar 2011; revised 25 Apr 2011; accepted 25 Apr 2011; published 17 May 2011

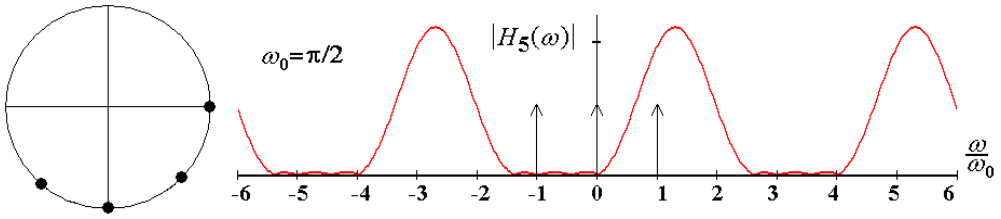

Fig. 2. Magnitude of $H_5(\omega)$, and its CP-diagram. The PSA spectrum, has been considerably flattened around $\pi/2$ with respect to $H_{SH}(\omega)$ for the same measured interferograms. From the CP-diagram alone, the spectral shape outside the 4 zeroes shown is absent. In contrast the plot of $|H_5(\omega)|$ shows it clearly. One must be aware of the small ripples within the stop-band.

In Fig. 3 we show an application for our modified PSA (Eq. (13)) to simulated speckle-like interferograms. For the sake of visual clarity we only show 3 interferograms (out of 5) along with the wrapped phase obtained from Eq. (13).

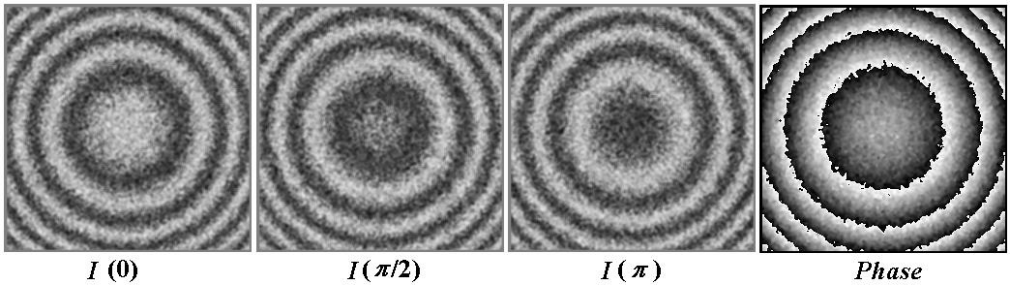

Fig. 3. Simulated speckle-like interferograms applied to our modified PSA (Eq. (13)). The 5 interferograms used in Eq. (13) may also be used for the *SH*-PSA. However the PSA detuning robustness is higher in our modified PSA (Eq. (13)) than in the *SH*-PSA (Eq. (11)).

Let us continue with another example, a 9-steps PSA. We want high detuning robustness, (6-zeroes) at ω_0=-π/2, and also robustness to bias illumination's variation; 2-zeroes at ω=0. In Fig. 4 the CP-diagram of $P_9(x)=(x-1)^2(x+i)^6$, and the plot of $|P_9(e^{i\omega})|$ are shown,

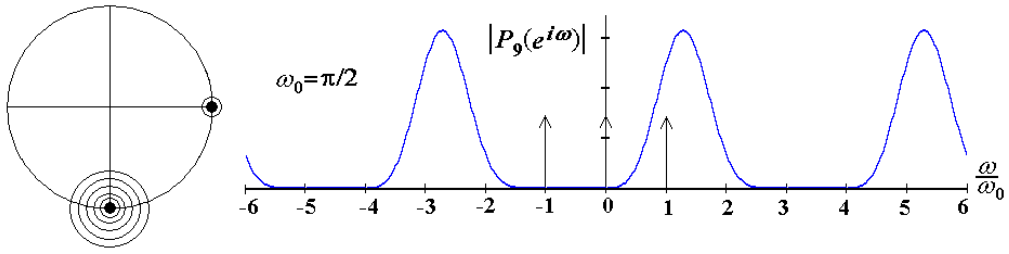

Fig. 4. Magnitude of $P_9(e^{i\omega})$ and its CP-diagram. The resulting spectral rejection band is wide (6^{th} order) around ω_0, and 2^{nd} order around the origin.

Let us widen even further $P_9(e^{i\omega})$ around -ω_0. A flatter than $P_9(e^{i\omega})$ spectral response is obtained by spreading-out its 8 available zeroes. This is done while gauging the $|H_9(\omega)|$ plot. After some trial-and-error iterations we settle on the following *non-symmetric* PSA,

$$H_9(\omega)=[1-e^{-i(\omega-0.3\omega_0)}][1-e^{i\omega}][1-e^{-i(\omega+0.3\omega_0)}][1-e^{-i(\omega+0.6\omega_0)}][1-e^{-i(\omega+\omega_0)}] \\ [1-e^{-i(\omega+1.4\omega_0)}][1-e^{-i(\omega+1.7\omega_0)}][1-e^{-i(\omega+2\omega_0)}]. \quad (14)$$

#143799 - $15.00 USD Received 7 Mar 2011; revised 25 Apr 2011; accepted 25 Apr 2011; published 17 May 2011

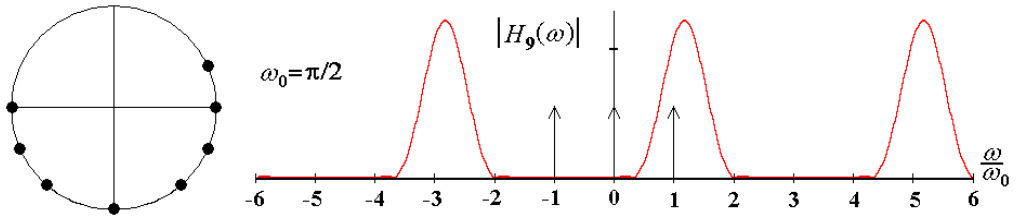

Fig. 5. CP diagram, and magnitude of $H_9(\omega)$. The resulting PSA' spectral shape has been further flattened, with respect to $P_9(e^{i\omega})$ around ω_0, and around of the origin. . From the CP-diagram alone, one may only wonder the spectral amplitude outside the zeroes shown, making almost impossible the fine-tuning task performed herein.

As Fig. 5 shows, we have further flattened the rejected-band with respect to that of $P_9(e^{i\omega})$. The 8 zeroes have been spread-out around the unit circle. The designer may widen even more the rejection-band at a cost of tolerating bigger ripples; the signal amplitude at ω_0 is 82 times bigger than the highest ripple. This plot clearly shows the detailed spectral amplitude including the small ripples which cannot be seen in the CP-diagram. Fourier-inverse transforming $H_9(\omega)$ we find $h_9(t)$ and from it, the searched 9-steps *non-symmetric* PSA.

5. Signal-to-Noise power ratio (S/N) in PSA designs

Given that the CP-diagram is blind to the continuous spectral' amplitude, we cannot see if our PSA would perform better against noise with a slight change of the data carrier ω_0. By looking at Fig. 5 (for example) we see that the desired signal at $\omega=\pi/2$, do not coincide with the spectra's peak. Let us compute the S/N power-ratio at ω_0, and at its peak $1.16\omega_0$ [12],

$$\text{S/ N}(\omega_0)=\frac{|H_9(\omega_0)|^2}{\frac{1}{2\pi}\int_{-\pi}^{\pi}|H_9(\omega)|^2\,d\omega}=5.3\,,\qquad \text{S/ N}(1.16\omega_0)=\frac{|H_9(1.16\omega_0)|^2}{\frac{1}{2\pi}\int_{-\pi}^{\pi}|H_9(\omega)|^2\,d\omega}=6.6. \quad (15)$$

That is, increasing our carrier ω_0 from 0.5π (radians/sample) to 0.58π one obtains a 24.5% gain in the S/N power-ratio, *i.e.* (6.6/5.3)=1.245. We have suggested this carrier increase because we can seen the continuous plot of $|H_9(\omega)|$ in Fig. 5. In contrast, observing the CP-diagram alone, it is impossible to see where the location of the PSA's spectral maximum is. Also, the F&K' spectral plot [4] cannot be used, because it does not exist for *non-symmetrical* PSAs.

6. Conclusions

We have presented a zero-based, fine-tuning, spectrum-shaping technique for designing *N*-steps PSAs, based on the visualization and gauging of its continuous FTF spectral magnitude $|H(\omega)|$. This technique gives more possibilities to approximate a target spectrum while keeping the size *N* of the PSA unchanged. This PSA's design method starts by specifying a desired PSA spectrum's template. Afterwards, the available (*N*-1) first-order zeroes are freely moved (fine-tuned), to approximate it. Finally, the inverse transform of the FTF ($h(t)$) is found, and from it the desired (in general non-symmetric) PSA. We remark, given that we freely move the PSA's (*N*-1) zeroes, we end-up (with probability 1) synthesizing *non-symmetric* PSAs. These non-symmetric PSAs cannot be analyzed using the F&K spectral-plotting technique.

Finally we remark that, the target PSA spectrum may be determined by taking the Fourier transform of actual interferometric measurements of the kind of fringes being analyzed. This real-data spectral estimation and the desired phase noise-rejection are the key to estimate how many samples *N* a given PSA needs, and also where its (*N*-1) zeroes may be located.

#143799 - $15.00 USD Received 7 Mar 2011; revised 25 Apr 2011; accepted 25 Apr 2011; published 17 May 2011